

A Nonlinear Research on Coupled Vibration of Strip Steel with the Impact of the Main Drive System of Tandem Mill

Chongyi Gao, Member, *IAENG*, Jianxiong Li, Le Liu and Li Wei

Abstract—Based on the movement mechanism of strip steel and main drive system during the continuous rolling process, the main drive system of each frame was simplified into a two-degree-of-freedom discrete model and the strip steel was simplified into an axially moving Euler beam. Then, the coupled mechanical model of transverse and longitudinal vibrations of the strip steel with torsional vibration of the main drive system was established. Meanwhile, the nonlinear vibration differential equations of the coupled model were derived with Hamilton's principle, and the solution method of the mathematical model was studied. In fact, the solution method of the mathematical model was a joint solution process of discrete matrix differential equations and continuous nonlinear differential equations. Therefore, the established model could be called the discrete-continuous coupled nonlinear vibration model. Then, the discrete-continuous coupled differential equations were jointly solved with the modified iteration method and the Kantorovich averaging method. Finally, by using the MATLAB simulation, the amplitude-frequency response curves of strip steel vibrations coupled with torsional vibration of main drive system were obtained to explore the influences of axial velocity and tension of strip steel on coupled vibration characteristics. The results improve the theoretical study on the vibration of rolling mill for engineering applications.

Index Terms—coupled model, nonlinear dynamics, strip steel vibration, torsional vibration

I. INTRODUCTION

During the continuous rolling process, strip steel vibrations are unavoidable [1]. The coupling between the elastoplastic body of strip steel and the main drive system

directly affects the overall dynamic performance of rolling mills, but the effect has not been widely concerned. The influences of the strip steel vibration and the torsional vibration of main drive system on the overall dynamic performance of rolling mills cannot be ignored. The coupling mechanism between the strip steel vibrations and the torsional vibration of main drive system is relatively complex and the coupled vibration may cause serious consequences [2]. Therefore, it is necessary to explore the nonlinear vibrations of strip steel with the impact of torsional vibration of the main drive system.

In recent years, the torsional vibration and strip steel vibration have been extensively researched. Liu Hongmin et al. found that the torsional vibration of rolling mills showed the chaotic characteristics [3]. Shi Peiming et al. obtained the amplitude frequency response equation of the nonlinear system under the combined action of motor disturbance torque and rolling load torque by using the multi-scale modeling method [4]. Zhang Yifang and Yan Xiaoqiang explored the coupling effects of the electric system on the torsional vibration of rolling mill transmission system [5]. Our group studied the influences of multi-clearance and slipping on the torsional vibration of the main drive system of rolling mill [6, 7]. In terms of strip steel vibrations, Swiatoniowski and Bar established the nonlinear vibration mathematical model based on the consideration of the coupling vibration effect between strip steel and adjacent frame systems and indicated the relationship between the rolling speed and the strip steel vibration [8, 9]. Kim et al. studied the parametric resonance of galvanized sheets in the process of metal plate coating, and analyzed the influences of axial velocity and time-varying tension on the plate's motion characteristics and stability [10]. Peng Yan and Sun Jianliang established the relationship model among front tension, back tension, and rolling force of the strip steel in the roller systems according to the relationship between the rolling speed and the angular velocity of the roll and gained the influence of the torsional vibration on the shape of the strip steel [11, 12]. Tong Chaonan et al. established the dynamic friction equation of the roll gap and the distribution model of the forward rolling stress in the deformation zone and discussed the vertical vibration mechanism and stability of the cold rolling mills [13].

Nevertheless, the coupling relationship between strip steel vibrations and torsional vibration of main drive system was seldom reported. We previously established a nonlinear dynamic coupling model between roller and strip steel [14, 15] and found that the torsional vibration of one frame main

Manuscript received June 4, 2018; revised August 12, 2019. This work was supported in part by the Natural Science Foundation of Hebei Province in China under Grant E2017203115, in part by the National Natural Science Foundation of China under Grant 61803327, in part by the Natural Science Foundation of Hebei Province in China under Grant F2016203263, and in part by the Youth Top-notch Project of Hebei Province under Grant BJ2019209.

C. Gao is currently a Lecturer with Department of Mechanical and Electrical Engineering, Tangshan University, Tangshan City, Hebei Province, China (e-mail: 7921086@163.com).

J. Li is currently an Associate Professor with Department of Automation, Yanshan University, Qinhuangdao City, Hebei Province, China (corresponding author to provide phone: 86-13833513655; fax: 86-335-8072979; e-mail: jxli@ysu.edu.cn).

L. Liu is currently a Lecturer with Department of Automation, Yanshan University, Qinhuangdao City, Hebei Province, China (e-mail: leliu@ysu.edu.cn).

L. Wei is currently a Lecturer with Department of Mechanical and Electrical Engineering, Tangshan University, Tangshan City, Hebei Province, China (e-mail: ysuweili@163.com).

drive system would transfer to the adjacent frame main drive system through the strip steel, thus resulting in the large-amplitude vibration of the roller through simulating the torsional vibration of main drive system of the each frame in finite element software [16]. In this paper, we explored the coupling relationship between transverse and longitudinal vibrations of strip steel with the impact of the torsional vibration of main drive system of tandem mill. The main drive system of the mill was simplified into a two-degree-of-freedom discrete system. Based on the axial moving beam theory [17], the strip steel was simplified into an axially moving Euler beam continuum, and a discrete-continuous coupled vibration model was established. Moreover, the modified iteration method and the Kantorovich averaging method were used to solve the discrete-continuous coupled differential equations [18]. The results can provide the important theoretical basis for controlling and analyzing the strip steel vibrations in the continuous rolling process.

II. MECHANICAL AND MATHEMATICAL MODELS

The main drive system of each frame in tandem mills can be regarded as a spring-mass discrete system composed of some rigid inertial elements and elastic elements. Then, the main drive system can be simplified into a 2-degree-of-freedom discrete model. The rotational inertia of each equivalent rotor are j_1 and j_2 , respectively. The connecting shaft is equivalent to an elastic component and the torsional stiffness of each shaft are k_1 and k_2 , respectively, as shown in Fig. 1. The strip steel is an elastic continuum whose width is much smaller than the length, and its bending stiffness is far less than the tensile stiffness. Based on the theory of axially moving beams, the strip steel is equivalent to an isotropic Euler beam continuum, and the strip steel and the main drive system of each frame are linked by the rollers. It is hypothesized that there is no relative movement between the rollers and that the strip steel and the upper and lower rollers are symmetrical, as shown in Fig. 2. The transverse displacement and longitudinal displacement are respectively $w(x_0, y_0, t)$ and $u(x_0, y_0, t)$; the rolling speed is v_0 ; the length of the strip steel between two adjacent frames is l ; The left and right tensions of strip steel are respectively P_1 and P_2 (let $P_1 = P_2 = P_0$).

According to the Hamilton principle, the mathematical model of the strip steel vibrations with the impact of the torsional vibration of main drive system is established. The kinematic energy T_1 of axially moving Euler beam can be written as

$$T_1 = \frac{1}{2} \int_0^l \rho A [(v_0 + u_t + v_0 u_{,x_0})^2 + (w_t + v_0 w_{,x_0})^2] dx_0 \quad (1)$$

where ρ is the density of strip steel; A is the cross-sectional area of Euler beam; u_t is the first-order partial derivative of $u(x_0, y_0, t)$ with respect to t ; w_t is the first-order partial derivative of $w(x_0, y_0, t)$ with respect to t ; $u_{,x_0}$ is the first-order partial derivative of $u(x_0, y_0, t)$ with

respect to x_0 ; $w_{,x_0}$ is the first-order partial derivative of $w(x_0, y_0, t)$ with respect to x_0 ; other similar symbols represent the same meaning.

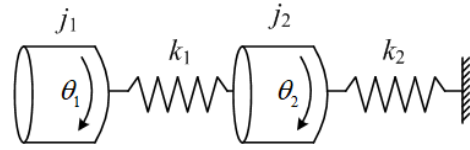


Fig. 1. Simplified model of the main drive system of a rolling mill

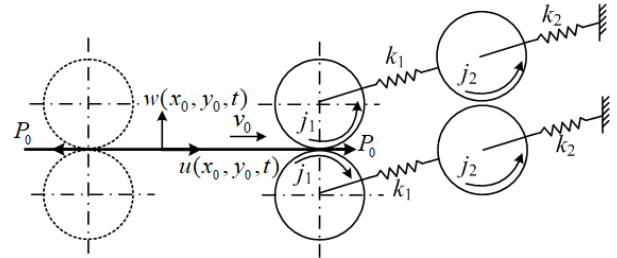


Fig. 2. Mechanical model of strip steel and main drive systems

The potential energy U_1 of Euler beam can be written as

$$U_1 = \frac{1}{2} \int_0^l [EA(u_{,x_0} + \frac{1}{2} w_{,x_0}^2)^2 + EIw_{,x_0x_0}^2] dx_0 \quad (2)$$

where E denotes the elastic modulus; I denotes the moment of inertia.

The kinetic energy of roller T_2 can be written as

$$T_2 = \frac{j_1}{2r^2} (u_t + v_0 u_{,x_0})^2 \quad (3)$$

where j_1 is the roller rotational inertia; r is the roller radius.

The potential energy U_2 of axial tension of Euler beam can be written as

$$U_2 = \int_0^l P_0 (u_{,x_0} + \frac{1}{2} w_{,x_0}^2) dx_0 \quad (4)$$

Then, based on Hamilton equation, we get:

$$\delta \int_{t_2}^{t_1} (T_1 + T_2 - U_1 - U_2) dt = 0 \quad (5)$$

After substituting Eqs. (1-4) into Eq. (5), the motion equations of strip steel with the influence of main drive system can be obtained as follows:

$$\begin{aligned} \rho A u_{,tt} + (\rho A v_0 - EA) u_{,x_0x_0} + 2\rho A v_0 u_{,x_0t} - EA w_{,x_0} w_{,x_0x_0} &= 0 \quad (6) \\ \rho A w_{,tt} + EI w_{,x_0x_0x_0x_0} + (\rho A v_0^2 - P_0) w_{,x_0x_0} & \\ + 2\rho A v_0 w_{,x_0t} - EA (w_{,x_0x_0} u_{,x_0} + u_{,x_0x_0} w_{,x_0} + \frac{3}{2} w_{,x_0}^2 w_{,x_0x_0}) &= 0 \quad (7) \end{aligned}$$

The boundary of the main drive system can be written as

When $x_0 = 0$,

$$[EAru_{,x_0} - P_0r] = -[j] \{\ddot{\theta}\} - [k] \{\theta\} \quad (8)$$

When $x_0 = l$,

$$[EAru_{,x_0} + P_0r] = -[j] \{\ddot{\theta}\} - [k] \{\theta\} \quad (9)$$

$$w(0) = w(l) = w_{,x_0x_0}(0) = w_{,x_0x_0}(l) = 0 \quad (10)$$

$$\begin{cases} w_{\max} = \phi_m \\ \frac{\partial^2 w(0,t)}{\partial x^2} - k \frac{\partial w(0,t)}{\partial x} = \frac{\partial^2 w(l,t)}{\partial x^2} + k \frac{\partial w(l,t)}{\partial x} = 0 \end{cases}$$

(11)

$$\text{where } [j] = \begin{bmatrix} j_1 & 0 \\ 0 & j_2 \end{bmatrix}; [k] = \begin{bmatrix} k_1 & -k_1 \\ -k_1 & k_1 + k_2 \end{bmatrix}; \{\theta\} = \begin{Bmatrix} \theta_1 \\ \theta_2 \end{Bmatrix};$$

$$\{\ddot{\theta}\} = \begin{Bmatrix} \ddot{\theta}_1 \\ \ddot{\theta}_2 \end{Bmatrix}.$$

Let $w = \varphi_0(x_0) \cos \omega_0 t$, $u = \phi_0(x_0) \cos^2 \omega_0 t$ can be got from Eq. (6). Then, after substituting w and u into Eqs. (7-11), the Kantorovich averaging method is applied to the interval $[0, 2\pi/\omega_0]$ and the motion equations are transformed as:

$$(\rho A v_0^2 - EA) \varphi_{0,x_0 x_0} - EA \phi_{0,x_0} \phi_{0,x_0 x_0} = 0 \quad (12)$$

$$EI \varphi_{0,x_0 x_0 x_0 x_0} + (\rho A v_0^2 - P_0) \varphi_{0,x_0 x_0} - \omega_0^2 \rho A \varphi_0 - \frac{3}{4} EA (\varphi_{0,x_0 x_0} \phi_{0,x_0} + \varphi_{0,x_0} \phi_{0,x_0 x_0} + \frac{3}{2} \varphi_{0,x_0}^2 \varphi_{0,x_0 x_0}) = 0 \quad (13)$$

The boundary of the main drive system can be written as when $x_0 = 0$,

$$\frac{4}{3} P_0 r^2 - EA r^2 = \frac{k_1 k_2}{(k_1 + k_2)} \phi_0 + \left[\frac{j_1 k_1 + j_1 k_2 - k_1 j_2}{(k_1 + k_2)} \right] (v_0^2 \phi_{0,x_0 x_0} - \frac{4}{3} \omega_0^2 \phi_0) \quad (14)$$

$$+ \frac{j_1 j_2}{(k_1 + k_2)} (v_0^4 \phi_{0,x_0 x_0 x_0 x_0} - 8 v_0^2 \omega_0^2 \phi_{0,x_0 x_0} - \frac{16}{3} \omega_0^4 \phi_0)$$

when $x_0 = l$,

$$-\frac{4}{3} P_0 r^2 - EA r^2 = \frac{k_1 k_2}{(k_1 + k_2)} \phi_0 + \left[\frac{j_1 k_1 + j_1 k_2 - k_1 j_2}{(k_1 + k_2)} \right] (v_0^2 \phi_{0,x_0 x_0} - \frac{4}{3} \omega_0^2 \phi_0)$$

$$+ \frac{j_1 j_2}{(k_1 + k_2)} (v_0^4 \phi_{0,x_0 x_0 x_0 x_0} - 8 v_0^2 \omega_0^2 \phi_{0,x_0 x_0} - \frac{16}{3} \omega_0^4 \phi_0)$$

(15)

$$\varphi_0(0) = \varphi_0(l) = \varphi_{0,x_0}(0) = \varphi_{0,x_0}(l) = 0 \quad (16)$$

$$\varphi_0\left(\frac{l}{2}\right) = \varphi_{0m} \quad (17)$$

For the convenience of calculation, the dimensionless quantities are introduced as follows:

$$x = \frac{x_0}{l}; \varphi = \frac{\varphi_0}{l}; \phi = \frac{\phi_0}{l}; v = v_0 \sqrt{\frac{\rho}{E}}; P = \frac{P_0 l^2}{EI};$$

$$\omega = \omega_0 \sqrt{\frac{\rho A l^4}{EI}}; S = \frac{A l^2}{I}; J_i = \frac{j_i}{\rho A r^2 l} \quad (i=1,2);$$

$$K_i = \frac{k_i l}{EA r^3} \quad (i=1,2).$$

Then, the dimensionless forms of Eqs. (12-17) can be respectively obtained:

$$(v^2 - 1) \phi_{,xx} - \varphi_{,x} \varphi_{,xx} = 0 \quad (18)$$

$$\varphi_{,xxxx} + S v^2 \varphi_{,xx} - \omega^2 \varphi - \frac{3}{4} S (\varphi_{,xx} \phi_{,x} + \varphi_{,x} \phi_{,xx} + \frac{3}{2} \varphi_{,x}^2 \varphi_{,xx}) = 0 \quad (19)$$

The boundary of the main drive system can be written as when $x_0 = 0$,

$$\frac{4P}{3S} - \phi_{,x} = \frac{K_1 K_2 r}{K_1 + K_2} \phi + \left[\frac{J_1 K_1 + J_1 K_2 - K_1 J_2}{K_1 + K_2} \right] (v^2 \phi_{,xx} - \frac{4\omega^2}{3S} \phi) + \frac{J_1 J_2}{(K_1 + K_2) r} (v^4 \phi_{,xxxx} - \frac{8v^2 \omega^2}{S} \phi_{,xx} - \frac{16\omega^4}{3S} \phi) \quad (20)$$

when $x_0 = l$,

$$-\frac{4P}{3S} - \phi_{,x} = \frac{K_1 K_2 r}{K_1 + K_2} \phi + \left[\frac{J_1 K_1 + J_1 K_2 - K_1 J_2}{K_1 + K_2} \right] (v^2 \phi_{,xx} - \frac{4\omega^2}{3S} \phi) + \frac{J_1 J_2}{(K_1 + K_2) r} (v^4 \phi_{,xxxx} - \frac{8v^2 \omega^2}{S} \phi_{,xx} - \frac{16\omega^4}{3S} \phi) \quad (21)$$

$$\varphi(0) = \varphi(l) = \varphi_{,x}(0) = \varphi_{,x}(l) = 0 \quad (22)$$

$$\varphi\left(\frac{l}{2}\right) = \varphi_m \quad (23)$$

III. SOLUTION OF VIBRATION EQUATIONS

Due to the difficulty of solving the mathematical model, the modified iteration method is adopted to solve Eqs. (18-23).

A. First-order approximate solution

Firstly, all the nonlinear terms in Eq. (19) are omitted and the equations can be simplified as:

$$\varphi_{1,xxxx} - \omega^2 \varphi_1 = 0 \quad (24)$$

The series solution of Eq. (24) is:

$$\varphi_1(x) = a_0 M_0(x) + a_1 N_0(x) + a_2 I_0(x) + a_3 K_0(x) \quad (25)$$

where, $M_0 = \sum_{n=0}^{\infty} \frac{(\omega^2)^n}{(4n)!} x^{4n}$; $N_0 = \sum_{n=0}^{\infty} \frac{(\omega^2)^n}{(4n+1)!} x^{4n+1}$;

$$I_0 = \sum_{n=0}^{\infty} \frac{(\omega^2)^n}{(4n+2)!} x^{4n+2}$$
; $K_0 = \sum_{n=0}^{\infty} \frac{(\omega^2)^n}{(4n+3)!} x^{4n+3}$.

Substituting $\varphi_1(x)$ into Eqs. (22-23) gives $\omega_1 = 16.71$. The coefficients of Eq. (25) are respectively:

$$a_0 = 0; a_1 = \mu_1 \varphi_m; a_2 = 0; a_3 = \mu_2 \varphi_m;$$

$$\text{where, } \mu_1 = \frac{-K_0(1)}{N_0(1)K_0(\frac{1}{2}) - N_0(\frac{1}{2})K_0(1)}$$
;

$$\mu_2 = \frac{N_0(1)}{N_0(1)K_0(\frac{1}{2}) - N_0(\frac{1}{2})K_0(1)}.$$

Thus,

$$\varphi_1(x) = \varphi_m \left[\mu_1 \sum_{n=0}^{\infty} \frac{\omega_1^{2n} x^{4n+1}}{(4n+1)!} + \mu_2 \sum_{n=0}^{\infty} \frac{\omega_1^{2n} x^{4n+3}}{(4n+3)!} \right] \quad (26)$$

Substituting $\varphi_1(x)$ into Eq. (18) gives

$$\phi_1 = \frac{1}{2(v^2 - 1)} \int \varphi_{1,x}^2 dx + c_1 x + c_2 \quad (27)$$

The coefficients c_1 and c_2 can be derived from the boundary Eqs. (20-21):

$$c_1 = -\frac{1}{Q_1} \left[\frac{J_1 J_2 v^4}{(v^2 - 1)(K_1 + K_2) r} (3\varphi_{1,xx} \varphi_{1,xxx} + \varphi_{1,x} \varphi_{1,xxxx}) + \frac{Q_2}{v^2 - 1} \varphi_{1,x} \varphi_{1,xx} + \frac{Q_1}{2(v^2 - 1)} \int \varphi_{1,x}^2 dx + \frac{1}{2(v^2 - 1)} \varphi_{1,x}^2 + \frac{8P}{3S} \right]_{x=l};$$

$$c_2 = \frac{1}{Q_1^2(v^2-1)} \left[\frac{J_1 J_2 v^4}{(K_1 + K_2)r} (3\varphi_{1,xx}\varphi_{1,xxx} + \varphi_{1,x}\varphi_{1,xxx}) \right. \\ \left. + Q_2\varphi_{1,x}\varphi_{1,xx} + \frac{Q_1}{2} \int \varphi_{1,x}^2 dx + \frac{8P(v^2-1)}{3S} + \frac{1}{2Q_1^2} \varphi_{1,x}^2 \right]_{x=1} + \frac{4P}{3SQ_1}$$

where,

$$Q_1 = \frac{K_1 K_2 r}{K_1 + K_2} - \frac{4(K_1 J_1 + K_1 J_2 + K_1 J_2)\omega^2}{3S(K_1 + K_2)} - \frac{16J_1 J_2 \omega^4}{3S^2 r(K_1 + K_2)}, \\ Q_2 = \frac{J_1 K_1 + J_2 K_2 - K_1 J_2}{K_1 + K_2} v^2 - \frac{8J_1 J_2 v^2 \omega^2}{rS(K_1 + K_2)}.$$

B. Second-order modified iterative solution

In the second-order iteration, substituting $\varphi_1(x)$ and $\dot{\varphi}_1(x)$ into Eq. (19) and omitting the non-linear terms, one gives

$$\varphi_{2,xxx} - \omega^2 \varphi_2 = \alpha \varphi_{1,xx} + \beta \varphi_{1,x}^2 \varphi_{1,xx} \quad (28)$$

$$\text{where, } \alpha = P + \frac{3}{4} S c_1 - S v^2; \quad \beta = \frac{9Sv^2}{8(v^2-1)};$$

$$\varphi_{1,x}^2(x) = \varphi_m^2 \left(\sum_{n=0}^{\infty} A_n^{(1)} x^{4n} + \sum_{n=0}^{\infty} B_n^{(1)} x^{4n+2} \right);$$

$$\varphi_{1,xx}(x) = \varphi_m \left(\sum_{n=1}^{\infty} C_n^{(1)} x^{4n-1} + \sum_{n=0}^{\infty} D_n^{(1)} x^{4n+1} \right).$$

where, $A_0^{(1)} = \mu_1^2$;

$$A_n^{(1)} = \sum_{n_1=0}^n \frac{\mu_1^2 \omega_1^{2n}}{(4n_1)!(4n-4n_1)!} + \sum_{n_1=0}^{n-1} \frac{\mu_2^2 \omega_1^{2n-2}}{(4n_1+2)!(4n-4n_1-2)!}; \\ (n=1,2,\dots)$$

$$B_n^{(1)} = \sum_{n_1=0}^n \frac{2\mu_1 \mu_2 \omega_1^{2n}}{(4n_1)!(4n-4n_1+2)!} \quad (n=0,1,\dots);$$

$$C_n^{(1)} = \frac{\mu_1 \omega_1^{2n}}{(4n-1)!} \quad (n=1,2,\dots);$$

$$D_n^{(1)} = \frac{\mu_2 \omega_1^{2n}}{(4n+1)!} \quad (n=0,1,\dots).$$

Then, the solution of Eq. (28) is written as:

$$\varphi_2(x) = \varphi_m \left[\zeta_1 \sum_{n=0}^{\infty} \frac{\omega^{2n} x^{4n+1}}{(4n+1)!} + \zeta_2 \sum_{n=0}^{\infty} \frac{\omega^{2n} x^{4n+3}}{(4n+3)!} \right] \\ + \varphi_m \left(\sum_{n=1}^{\infty} A_n x^{4n-1} + \sum_{n=0}^{\infty} B_n x^{4n+1} \right) \\ + \varphi_m^3 \left(\sum_{n=1}^{\infty} C_n x^{4n-1} + \sum_{n=0}^{\infty} D_n x^{4n+1} + \sum_{n=0}^{\infty} E_n x^{4n+3} \right) \quad (29)$$

where, $A_1 = B_0 = C_1 = D_0 = E_0 = 0$;

$$A_{n+1} = \frac{\omega^2 A_n + \alpha C_n^{(1)}}{(4n+3)(4n+2)(4n+1)4n};$$

$$B_{n+1} = \frac{\omega^2 B_n + \alpha D_n^{(1)}}{(4n+5)(4n+4)(4n+3)(4n+2)};$$

$$C_{n+1} = \frac{\omega^2 C_n + \beta A_n^{(2)}}{(4n+3)(4n+2)(4n+1)4n};$$

$$D_{n+1} = \frac{\omega^2 D_n + \beta B_n^{(2)}}{(4n+5)(4n+4)(4n+3)(4n+2)};$$

$$E_{n+1} = \frac{\omega^2 E_n + \beta C_n^{(2)}}{(4n+7)(4n+6)(4n+5)(4n+4)}.$$

Substituting $\varphi_2(x)$ into Eqs. (22-23) gives:

$$A \xi = 0 \quad (30)$$

$$\text{where, } \zeta = [\zeta_1 \quad \zeta_2 \quad 1]^T; \quad A = \begin{bmatrix} a_{11} & a_{12} & a_{13} \\ a_{21} & a_{22} & a_{23} \\ a_{31} & a_{32} & a_{33} \end{bmatrix};$$

$$a_{11} = \sum_{n=0}^{\infty} \frac{\omega^{2n}}{(4n+1)!}; \quad a_{21} = \sum_{n=0}^{\infty} \frac{\omega^{2n}}{(4n+1)!} \left(\frac{1}{2}\right)^{4n+1};$$

$$a_{31} = \sum_{n=1}^{\infty} \frac{\omega^{2n}}{(4n-1)!}; \quad a_{12} = \sum_{n=0}^{\infty} \frac{\omega^{2n}}{(4n+3)!};$$

$$a_{22} = \sum_{n=0}^{\infty} \frac{\omega^{2n}}{(4n+3)!} \left(\frac{1}{2}\right)^{4n+3}; \quad a_{32} = \sum_{n=0}^{\infty} \frac{\omega^{2n}}{(4n+1)!};$$

$$a_{13} = \left(\sum_{n=1}^{\infty} A_n + \sum_{n=0}^{\infty} B_n \right) + \varphi_m^2 \left(\sum_{n=1}^{\infty} C_n + \sum_{n=0}^{\infty} D_n + \sum_{n=0}^{\infty} E_n \right);$$

$$a_{23} = \left(\sum_{n=1}^{\infty} A_n \left(\frac{1}{2}\right)^{4n-1} + \sum_{n=0}^{\infty} B_n \left(\frac{1}{2}\right)^{4n+1} \right)$$

$$+ \varphi_m^2 \left[\sum_{n=1}^{\infty} C_n \left(\frac{1}{2}\right)^{4n-1} + \sum_{n=0}^{\infty} D_n \left(\frac{1}{2}\right)^{4n+1} + \sum_{n=0}^{\infty} E_n \left(\frac{1}{2}\right)^{4n+3} \right] - 1;$$

$$a_{33} = \left(\sum_{n=1}^{\infty} (4n-1)(4n-2)A_n + \sum_{n=0}^{\infty} (4n+1)4nB_n \right)$$

$$+ \varphi_m^2 \left[\sum_{n=1}^{\infty} (4n-1)(4n-2)C_n + \sum_{n=0}^{\infty} (4n+1)4nD_n \right]$$

$$+ \sum_{n=0}^{\infty} (4n+3)(4n+2)E_n \quad]$$

The analytic expression of vibration frequency ω_2 is obtained by $\det A = 0$, then, the second-order modified iterative solution is determined.

IV. CALCULATION CASE AND DISCUSSION

GL-E36 strip steel between F2 and F3 frames of a mill is selected to simulate the rolling process by Matlab. The main parameters are listed as follows. The thickness of strip steel h is 18 mm; the dimensionless tension P is 1×10^4 ; the rotational inertia of each equivalent rotor is $J_1 = 800$, $J_2 = 600$; the torsional stiffness of each shaft section is $K_1 = 6 \times 10^4$, $K_2 = 8 \times 10^4$. The influences of the amplitude φ_m on the vibration frequency under the dimensionless axial velocities of 2×10^{-3} , 6×10^{-3} , 10×10^{-3} , and 14×10^{-3} is displayed in Fig. 3. The vibration frequency of strip steel rises with the increase of the amplitude, and the vibration performance shows positive correlation. Moreover, when the axial velocity v is smaller, the amplitude has the greater impact on the vibration frequency. When the axial velocity continues to increase, the curve gradually tends to be flat. This phenomenon indicates that the greater the strip rolling

speed is, the smaller the influence of the amplitude of the strip steel on the vibration frequency is. The higher rolling speed within a certain range will also increase economic benefits in production practices.

Fig. 4 displays the dimensionless amplitude-frequency response curves under the different tensions of strip steel. The dimensionless axial velocity $v=1 \times 10^{-2}$; the rotational inertia of each equivalent rotor is $J_1 = 800$, $J_2 = 600$; the torsional stiffness of each shaft section is $K_1 = 6 \times 10^4$, $K_2 = 8 \times 10^4$; the dimensionless tension P are respectively 1×10^4 , 2×10^4 , 3×10^4 and 4×10^4 . The vibration frequency rises gradually with the increase of the amplitude, and the response curves intersect at the point $\varphi_m \approx 0.023$. Under the lower amplitude condition, the tension of strip steel shows the insignificant effect on the vibration frequency. When $\varphi_m \geq 0.023$, the tension influences the vibration frequency greatly. In addition, with the increase of the tension, the rising trend of amplitude-frequency curves decreases obviously. That is to say, the larger the tension is, the more stable the vibration of strip steel is.

In theoretical modeling, equivalent rotor 1 of the main drive system is the closest to the strip steel. Therefore, the influence of the rotational inertia on the strip steel vibrations cannot be neglected. When the rotational inertia of equivalent rotor 1 is changed, it will show a restraint effect on various factors of the strip steel vibrations.

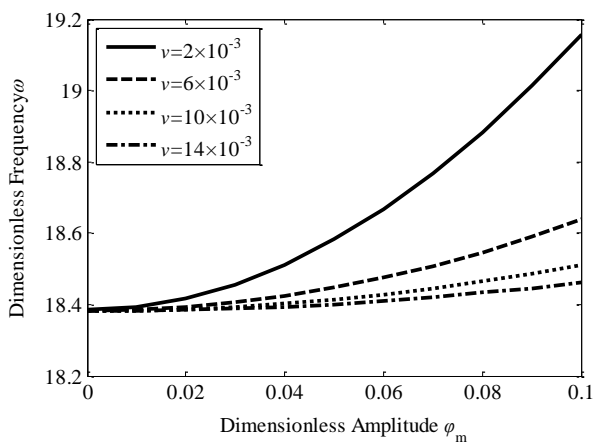


Fig. 3. Dimensionless amplitude-frequency response curves under different axial speeds

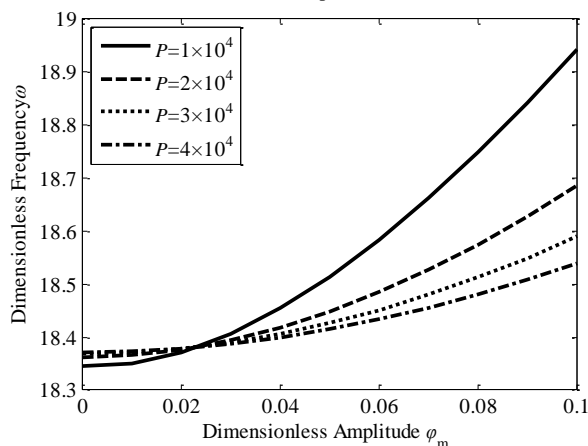


Fig. 4. Dimensionless amplitude-frequency response curves under different tensions

Fig. 5 shows the relationship between the frequency and the tension of strip steel under different conditions of rotational inertia J_1 . As shown in Fig. 5, the dimensionless amplitude is $\varphi_m = 0.06$; the dimensionless axial velocity of strip steel $v=1 \times 10^{-2}$; the dimensionless rotational inertia of the equivalent rotor 2 $J_2 = 600$; the dimensionless torsional stiffness of each shaft section is $K_1 = 6 \times 10^4$, $K_2 = 8 \times 10^4$. The influence of the tension of strip steel on the vibration frequency under the rotational inertia J_1 of 200, 400, 600 and 800 is illustrated. The vibration frequency decreases with the increase in the tension of strip steel. When $P \leq 2 \times 10^4$, the tension has the great effect on the vibration frequency; when the tension continues to increase, the vibration of strip steel tends to be stable. In addition, when the rotational inertia increases, the vibration frequency increases gradually, but the increasing degree decreases gradually. When the rotational inertia increases to a certain value, the boundary of strip steel is close to the fixed condition. That is to say, when the rotational inertia is large, the influence of the change in the rotational inertia on the $P-\omega$ relationship curves is gradually weakened.

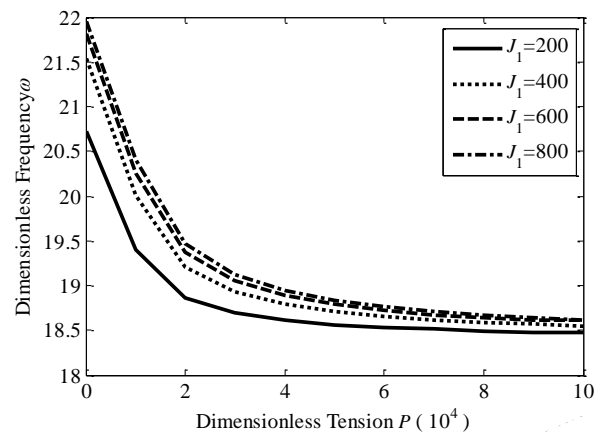


Fig. 5. Relationship between tension and frequency under different rotational inertias

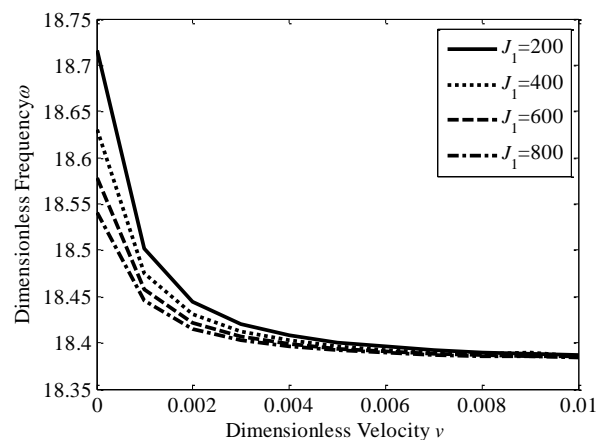


Fig. 6. Relationship between velocity and frequency under different rotational inertias

Fig. 6 shows the relationship curves between the frequency and the axial velocity under different conditions of rotational inertia J_1 . In Fig. 6, the dimensionless amplitude

$\varphi_m = 0.06$; the dimensionless rotational inertia of equivalent rotor 2 $J_2 = 600$; the dimensionless torsional stiffness of each shaft section is $K_1 = 6 \times 10^4$, $K_2 = 8 \times 10^4$. The influence of axial velocity on vibration frequency, under the rotational inertias J_1 of 200, 400, 600 and 800 is shown. With the increase of the axial velocity, the vibration frequency of strip steel decreases gradually. When $v \leq 2 \times 10^{-3}$, the downward trend of the relationship curves $v - \omega$ is obvious, and the axial velocity has a great effect on the vibration frequency. When the velocity continues to increase, the vibration frequency curves gradually show the consistent trend. The declining trend of the relationship curves $v - \omega$ is more significant when the rotational inertia is smaller. In other words, the smaller rotational inertia near the roller end has the greater impact on the $v - \omega$ curves.

V. CONCLUSION

The motion state of the strip steel and the main drive systems during the rolling process was simulated in the study. The torsional vibration of the main drive system was simplified as a two-degree-of-freedom discrete model, and the strip steel vibrations were simplified as a transverse and longitudinal vibrations model of Euler beam. The mechanical model and mathematical model of discrete-continuous coupled model were then established based on roller coupling. Then, the analytical solution of the coupled vibration equations were solved by the modified iteration method and the Kantorovich averaging method.

The amplitude-frequency responses of the strip steel vibration were analyzed based on the consideration of the different axial velocities and tensions of strip steel. The influences of axial velocity and tension of strip steel on the vibration frequency were discussed under different rotational inertias near the roller end. The larger rotational inertia had the greater impact on the $P - \omega$ curves and the smaller effect on the $v - \omega$ curves. Furthermore, with the infinite increase of the related vibration factors, the curves tend to be flat and the strip steel boundary tends to be fixed.

REFERENCES

- [1] L. J. Sun, C. Shao and L. Zhang, "Hybrid dynamic continuous strip thickness prediction of hot rolling," *Engineering Letters*, vol. 35, no. 3, pp. 268-276, 2017.
- [2] X. B. Fan, Y. Zang and F. Wang, "Hot strip mill nonlinear torsional vibration with multi-stand coupling," *Journal of Vibroengineering*, vol. 17, no. 4, pp. 1623-1633, 2015.
- [3] Y. Z. Shen, H. M. Liu and J. Xiong, "Analysis of chaotic behavior of the main drive system with clearance of a heavy plate mill," *Engineering Mechanics*, vol. 27, no. 7, pp. 232-236, 2010.
- [4] P. M. Shi, K. L. Xia and B. Liu, "Non-main resonance characteristics of nonlinear torsional vibration of rolling mill's multi-degree-of-freedom main drive system," *Journal of Vibration and Shock*, vol. 34, no. 12, pp. 35-41, 2015.
- [5] Y. F. Zhang, X. Q. Yan and Q. H. Lin, "Characteristic of torsional vibration of mill main drive excited by electromechanical coupling," *Chinese Journal of Mechanical Engineering*, vol. 29, no. 1, pp. 180-187, 2016.
- [6] C. Y. Gao, G. J. Du and Z. J. Zhang, "Torsional vibration analysis of the main drive system of a rolling mill with impact of multiclearance" *Journal of Mechanical Engineering*, vol. 50, no. 3, pp. 130-136, 2014.
- [7] G. J. Du, Z. J. Zhang and C. Y. Gao, "Torsional vibration of main drive system with impact of slipping and two-clearance of a heavy plate mill," *Iron and Steel*, vol. 48, no. 2, pp. 39-43, 2013.

- [8] A. Swiatonowski and A. Bar, "Parametrical excitement vibration in tandem mills-mathematical model and its analysis," *Journal of Materials Processing Technology*, vol. 134, no. 2, pp. 214-224, 2003.
- [9] A. Bar and A. Swiatonowski, "Interdependence between the rolling speed and non-linear vibrations of the mill system," *Journal of Materials Processing Technology*, vol. 155, no. 1, pp. 2116-2121, 2004.
- [10] C. H. Kim, N. C. Perkins and C. W. Lee, "Parametric resonance of plates in a sheet metal coating process," *Journal of Sound and Vibration*, vol. 268, no. 4, pp. 679-697, 2003.
- [11] J. L. Sun, M. Zhang and Y. Peng, "Torsional vibration of 6-h rolling mill based on continuum dynamics and its relationship with strip quality," *Engineering Mechanics*, vol. 31, no. 4, pp. 239-244, 2014.
- [12] J. L. Sun, Y. Peng and H. M. Liu, "Dynamic characteristics of cold rolling mill and strip based on flatness and thickness control in rolling process," *Journal of Central South University*, vol. 21, no. 2, pp. 567-576, 2014.
- [13] X. Yang, Q. Li and C. N. Tong, "Vertical vibration mechanism analysis of aluminum cold rolling mills based on the dynamic friction equation in roll gap," *Journal of University of Science and Technology Beijing*, vol. 36, no. 1, pp. 104-109, 2014.
- [14] C. Y. Gao, G. J. Du and J. X. Li, "Nonlinear vibration of strip steel under inertial boundary conditions," *Journal of Vibration and Shock*, vol. 35, no. 1, pp. 5-10, 2016.
- [15] C. Y. Gao, G. J. Du, Y. Feng and J. X. Li, "Nonlinear vibration analysis of moving strip with inertial boundary condition," *Mathematical Problems in Engineering*, vol. 2015, no. 8, pp. 1-9, 2015.
- [16] C. Y. Gao, G. J. Du and J. X. Li, "Numerical analysis on torsional vibration of main driving system of rolling mill with strip steel," *Journal of Yanshan University*, vol. 40, no. 1, pp. 58-65, 2016.
- [17] L. Q. Chen and X. D. Yang, "Steady-state response of axially moving viscoelastic beams with pulsating speed: comparison of two nonlinear models," *International Journal of Solids and Structures*, vol. 42, no. 1, pp. 37-50, 2005.
- [18] L. L. Wang, "Periodic solutions for some strongly nonlinear oscillators applying he's methods," *IAENG International Journal of Applied Mathematics*, vol. 48, no. 4, pp. 368-372, 2018.



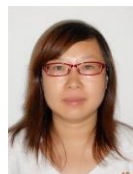
Chongyi Gao (M'18) was born in 1986 at Qinhuangdao of China. She received PhD degree in College of Civil Engineering and Mechanics from Yanshan University, Qinhuangdao, China, in 2016, then continued postdoctoral study at College of Mechanical Engineering from Yanshan University. Now she works at Mechanical and Electrical Engineering Department from Tangshan University. Her current research interests include nonlinear theory and application, rolling mill vibration and control.



Jianxiong Li was born in 1980 at Dingzhou of China. He received PhD degree in School of Electrical Engineering from Yanshan University, Qinhuangdao, China, in 2012. Now He works at School of Electrical Engineering from Yanshan University. His current research interests include rolling mill vibration and control, automation control and application.



Le Liu was born in 1985 at Shijiazhuang of China. He received PhD degree in School of Electrical Engineering from Yanshan University, Qinhuangdao, China, in 2015. Now He works at School of Electrical Engineering from Yanshan University. His current research interests include rolling mill vibration and control, automation control and application.



Li Wei was born in 1981 at Hengshui of China. She received M. E. degree in School of Electrical Engineering from Yanshan University, Qinhuangdao, China, in 2007. Now She works at School of Mechanical and Electrical Engineering Department from Tangshan University. Her current research interests include rolling mill vibration signal measurement.